Small angle neutron scattering from D_2O in the critical region

2000 J. Phys.: Condens. Matter 12 3531

(http://iopscience.iop.org/0953-8984/12/15/303)

J. Phys.: Condens. Matter **12** (2000) 3531–3542. Printed in the UK PII: S0953-8984(00)11280-9

Small angle neutron scattering from D_2O in the critical region

D M Sullivan†‡, G W Neilson‡¶, H E Fischer§ and A R Rennie‖

† Institut Laue–Langevin, 6 rue J Horowitz, 38042 Grenoble, France
‡ H H Wills Physics Laboratory, University of Bristol, Tyndall Avenue, Bristol, UK
§ Laboratoire LURE, Centre Universitaire Paris-Sud, BP 34, 91898 Orsay, France
‖ Department of Chemistry, Kings College, London, UK

Received 26 January 2000

Abstract. Small angle neutron scattering experiments were carried out on D_2O on the critical isochore. Apparatus was used which enabled the control of temperature to ± 0.01 K and pressure to 10 mbar. The corrected scattering data were used to extract values for the correlation length of the critical density fluctuations, ξ, and the thermodynamic limit of the structure factor, $S(0)$. Both quantities are found to show divergent power-law behaviour with reduced temperature, and have exponents $\nu = 0.62 \pm 0.03$ and $\gamma = 1.14 \pm 0.05$, respectively. These results confirm that D_2O belongs to the three-dimensional Ising universality class.

A value of $\xi_0 = 1.30 \pm 0.23$ Å was calculated for the characteristic correlation length of D_2O, a result that compares favourably with that inferred from thermodynamic data and calculated theoretically.

1. Introduction

The critical point of a single-component classical fluid is defined by the critical temperature, T_c, pressure, p_c, and density, ρ_c, and represents the thermodynamic state at which coexisting liquid and gas phases become indistinguishable. Above the critical temperature there can be no liquid–gas coexistence. The critical region of fluids has been the focus of much interest in the past few decades [1]. Theoretical studies based on the renormalization group have been successful in classifying the critical behaviour of various general fluids [2], and experimental work has provided useful information which has helped to characterize many material properties, and enable critical fluids to be used in commercially important processes such as the decaffeination of coffee and the optimization of chemical reactions [3].

The critical point denotes a singularity in the thermodynamic behaviour. When the critical point is approached from any direction on the phase diagram, divergent behaviour is shown in those thermodynamic quantities that are second-order derivatives of the free energy. The equation of state, asymptotically close to the critical point, takes a simple scaling form in terms of reduced state variables. The critical exponents describing this scaling behaviour are found to be a characteristic of the universality class to which the fluid belongs. The classification depends on the general type of interaction between particles and not on the chemical composition of the fluid [1].

Of particular relevance to the work described in this paper is the phenomenon of critical opalescence which can be spectacularly demonstrated in the scattering of light on a few systems at near-ambient conditions [4]. This phenomenon is caused by the thermal density fluctuations

¶ Reprint requests to G W Neilson.

0953-8984/00/153531+12$30.00

of atoms or molecules in a system near its critical point. As the critical point is approached along the critical isochore, the correlation length, ξ, associated with the collective behaviour of the atoms or molecules diverges according to a particular power law relationship. For example, in the case of a dipolar fluid in three dimensions, ξ diverges with a critical exponent $\nu = 0.630$, consistent with the 3D Ising universality class [1, 5].

It is with this background that we have undertaken a small angle neutron scattering (SANS) experiment to determine the critical opalescence in heavy water. Besides the obvious interest in water as a universal solvent medium for many biological and chemical processes, it can also be regarded as the prototypical hydrogen bonding liquid. Our motivation therefore is to extend our knowledge of the critical behaviour of this substance and confirm previous critical point work, which shows that water is a member of the 3D. Ising universality class [5]. In particular, our experimental results below provide the first direct determination of the characteristic correlation length and critical exponent of the fluid. A secondary aspect of our work is to assess the feasibility of studying opalescence in salt–water mixtures and ionic systems generally. Recent experiments on turbulence in ionic salts shows the intriguing situation of a delayed crossover from the Ising type of power-law behaviour close to the critical point to mean field far from the critical point [6]. One advantage of working on water is that the phase diagrams of both water (H_2O) and heavy water (D_2O) are well established, and several experimental properties have been measured in the critical regime of water [5, 7]. Kamgar-Parsi *et al* [7] previously determined the following critical parameters for D_2O: $T_c = 643.89 \pm 0.10$ K, $P_c = 216.71 \pm 0.05$ bar, $\rho_c = 356.2 \pm 2.5$ kg m^{-3}.

There are three possible scattering methods that can, in principle, be used to study critical opalescence: light scattering, small angle x-ray scattering (SAXS) and small angle neutron scattering (SANS). We have chosen the SANS technique for the range of momentum transfer that can be attained, the less restrictive constraints on the size and material of the sample container and the sensitivity to correlations in the structure of materials containing elements with low atomic numbers.

The choice of D_2O over H_2O is made purely on the basis of the preferential neutron scattering properties of the former that enables more accurate determination of the structure. In terms of the underlying physics we would anticipate no difference in critical behaviour of these two isotopically different materials.

The theory of critical fluctuations, due to Ornstein–Zernike, predicts the following equation for the structure factor [1] in terms of momentum transfer, Q, defined by the equation $Q = 4\pi(\sin\theta)/\lambda$, where θ is the scattering angle and λ is the incident wavelength:

$$S(Q) = S(0)/(1 + \xi^2 Q^2). \tag{1}$$

In this theory, ξ is the correlation length of the system. The equation is valid for small momentum transfers ($Q \ll \xi^{-1}$). Very close to the critical point, this condition is not accessible to experiment and equation (1) must be replaced by an expression featuring the Fisher-type decay of the correlations, described below.

For a pure one-component fluid, $S(0)$ is simply related to the isothermal compressibility, $\kappa_T = -V^{-1}(\partial V/\partial p)_T$:

$$S(0) = k_B T n \kappa_T \tag{2}$$

where n is the microscopic atomic number density [8].

Hence, by interpreting experimental structure factors in terms of equation (1) and equation (2) we obtain quantities for the correlation length and isothermal compressibility, both of which show divergent power-law behaviour in the critical regime. In particular, on the critical isochore above T_c the following power-law relations are expected:

$$\xi = \xi_0 t^{-\nu} \tag{3}$$

$$\kappa_T = p_c^{-1}\Gamma t^{-\gamma} \tag{4}$$

where γ, ν are critical exponents (an indication of the universality class of the fluid); ξ_0, Γ are amplitudes specific to the fluid and t is the reduced temperature:

$$t = (T - T_c)/T_c.$$

It can be seen from equation (1) that plotting $S(Q)^{-1}$ against Q^2 will give a straight line. When experimental data are shown in this way, it is known as an Ornstein–Zernike plot.

Since the correlation length is expected to diverge according to equation (3), for small values of reduced temperature, t, the condition of validity ($Q \ll \xi^{-1}$) for the Ornstein–Zernike equation may not be met by all momentum transfers in a given experimental range. In this regime, equation (1) must be replaced by a more accurate description of the decay of the correlations in real space. The correct form of this decay, at the critical point, is characterised by the Fisher exponent, η [9], which is defined in terms of the exponents in equation (3) and equation (4) by the relation $\gamma = \nu(2 - \eta)$.

The value for η is of the order of 0.02, and its determination represents a major challenge to the experimentalist. An experiment to determine η by SANS methods, such as that of Damay *et al* [10], must be performed far from the regime in which the Ornstein–Zernike equation is valid. In the present experiment our main objective is to measure the critical amplitudes and exponents in equation (3) and equation (4). Consequently, we have chosen to collect data predominately in a range of t and Q ($0.0003 < t < 0.02$, 0.008 Å$^{-1} < Q < 0.068$ Å^{-1}) in which the Ornstein–Zernike equation is valid, thereby allowing the determination of both ξ_0 and $S(0)$. This means that our data are not suitable for an extraction of the value of η.

A scaled equation of state for D_2O in the critical region has previously been defined by Kamgar-Parsi *et al* [7] with reference to thermodynamic measurements. We may use the properties of this equation of state, asymptotically close to the critical point, to predict the power-law behaviour of ξ and κ_T. In the case of the description of the correlation length we must apply the hypothesis of two-scale factor universality [1]. This hypothesis enables us to predict ξ_0 from the singular component of the free energy density in the equation of state [7], via the dimensionless theoretical constant $R_\xi^+ = 0.27 \pm 0.01$, cited in Privman *et al* [11]. The predictions for both amplitudes, with the associated exponents from [7], are as follows:

$$\xi_0 = 1.28 \text{ Å} \qquad \nu = 0.630$$
$$k_B T_c n_c p_c^{-1}\Gamma = 0.802 \qquad \gamma = 1.242$$

where n_c is the *atomic* number density at the critical point.

2. Sample control equipment

Figure 1 shows a layout of the apparatus used and includes an expanded view of the sample container. The pressure cell was designed to minimize temperature gradients across the sample. The beam passes through an aperture in the titanium sample container, which has a volume of 2.2 cm^3, a 2 mm path-length and 3mm windows. This is housed in an Inconel body (a nickel superalloy), which contains the heating and thermometry system.

A two-stage heating system was employed with the majority of heating power delivered at the circumference of the cell and two small cartridge heaters fitted in the cell body for fine temperature control. A four-wire platinum resistance thermometer fed to an AC bridge was used to measure temperature.

In order to contain the sample above the critical pressure we used a cell many times the mass of the sample. Due to the difficulty in placing a thermometer near to the sample in the neutron beam, there was a large systematic error in the measurement of sample temperature

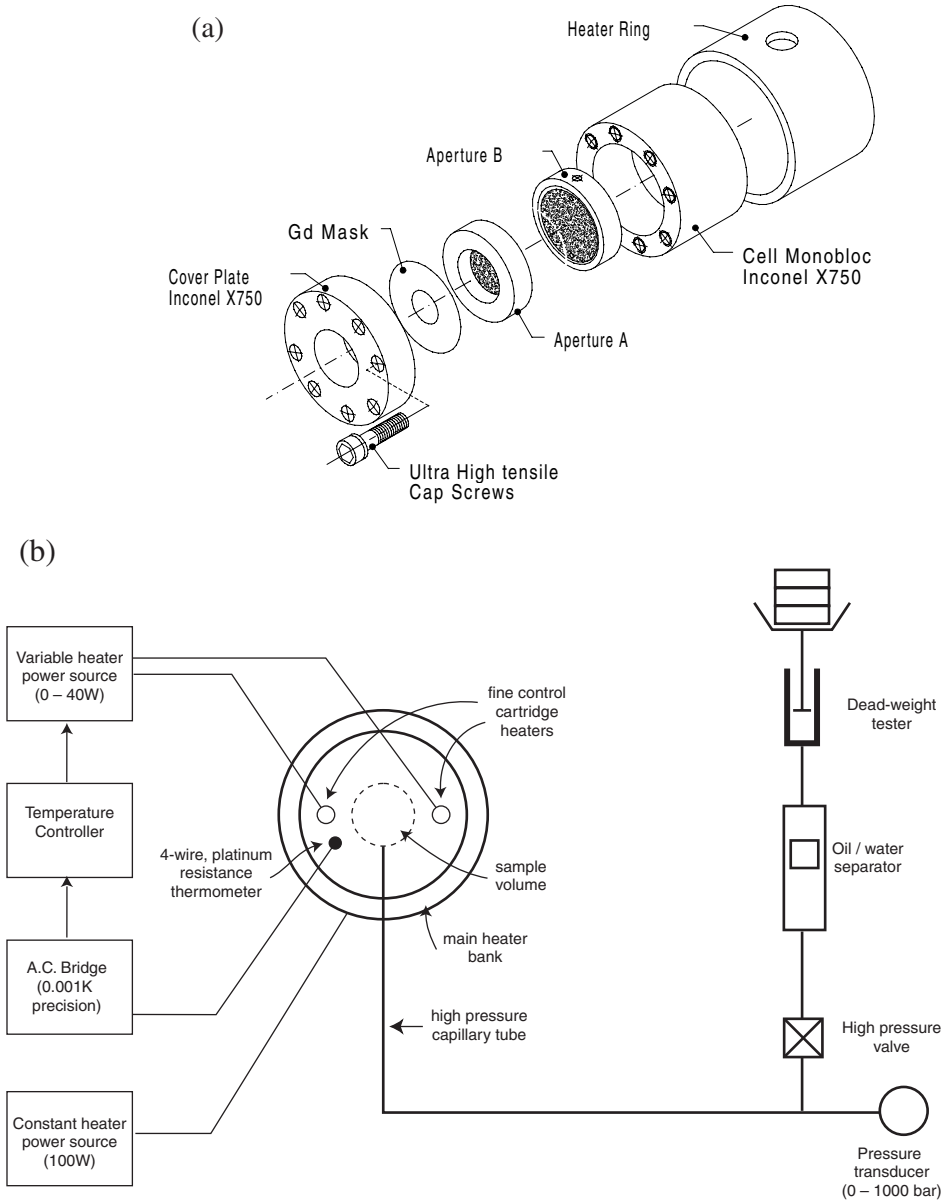

Figure 1. (a) Exploded view of sample container. (b) Schematic view of sample environment.

(about 0.17 K) although the actual temperature gradient across the sample was small (about 0.07 K). Moreover, time constraints required us to ramp the sample temperature continually, rather than take a series of points at steady state. The rate of heating strongly affected the difference between measured temperature and sample temperature. Such systematic errors prevented us from obtaining an independent measurement of the absolute critical temperature. Instead, we report our findings in terms of a reduced temperature, t, that is consistent and reproducible with measurements of the sample pressure, previous volumetric measurements and the sample scattering itself. See section 5 for more details on the calculation of t.

The sample volume was connected to the external pressurising system by a 1/16 inch o.d. (1/64 inch i.d.) high-pressure capillary tube. This enabled a pressure transducer, external to the cell, to make continual readings of the sample pressure. A dead-weight tester that used oil as a pressuring fluid applied pressure to the D_2O system (via an intermediate separator piston). The separator and dead-weight tester could be isolated from the sample volume and pressure transducer by closing a needle-type pressure valve.

3. Data acquisition

Prior to the SANS experiments on the critical isochore it was necessary to set precisely the density of the fluid. We found it best to locate the critical density by carefully setting the temperature and pressure just above the point at which the sample scatters most strongly, then sealing the cell. This required precise control of temperature (± 0.01 K) and pressure (± 10 mbar). By definition, a fluid close to the critical point is highly compressible so a dead-weight tester is employed to apply pressure. This device defines the pressure in the system by the principle of applying a known weight to a piston of known area.

Small angle neutron scattering measurements were taken on D22 (ILL, France) at a wavelength of $\lambda = 6$ Å, and a sample–detector distance of 10 m, giving an observable range of momentum transfer from 0.008 $Å^{-1}$ to 0.068 $Å^{-1}$. The D_2O sample was 99.9% atomic purity supplied by Sigma. The temperature of the system was varied continuously at a rate of approximately 0.1 K min^{-1}. Data were collected in 30 s acquisitions. We found that this gave sufficiently accurate data for the determination of the correlation length, $\xi(t)$ and long-wavelength limit of the structure factor, $S(0, t)$, as a function of reduced temperature, t.

4. Data analysis

The neutron counts measured at the 2D multidetector were grouped into incremental ranges of scattering angle, θ, which were each denoted by a value of Q, the mean elastic momentum transfer calculated for that range of angles.

The scattering measurements taken were: the sample and pressure cell at each state point, $I_{SC}(Q, t)$; the empty pressure cell, $I_C(Q)$; a 1 mm path-length H_2O sample at ambient conditions with fused quartz container, $I_{H_2O+SiO_2}(Q)$; and the empty fused quartz container, $I_{SiO_2}(Q)$. All measurements were normalized to the beam monitor counts.

The following expression was assumed for $I_{SC}(Q, t)$ in terms of $S(Q, t)$, the structure factor at reduced temperature, t, convoluted by the instrument resolution function:

$$I_{SC}(Q,t) = \Phi(Q)\left(A_{S,SC}N_{D_2O}\frac{\sigma_{coh}}{4\pi}S(Q,t) + M_{SC}\right) + \frac{A_{C,SC}}{A_{C,C}}I_C(Q) \qquad (5)$$

where N_{D_2O} is the total number of D_2O molecules in the neutron beam (calculated from the expected density of D_2O at the critical point); σ_{coh} is the coherent scattering cross section per atom of D_2O (defined in terms of the mean scattering lengths of the nuclei, $\sigma_{coh} = 4\pi\{\frac{2}{3}\bar{b}_D + \frac{1}{3}\bar{b}_o\}^2$); $A_{S,SC}$, $A_{C,SC}$ and $A_{C,C}$ are the relevant Paalman–Pings attenuation coefficients [12]; and M_{SC} is an isotropic component of the scattering cross-section due to multiple and incoherent scattering effects. The distribution $\Phi(Q)$ relates the measured counts (over the range of scattering angles corresponding to momentum transfer Q) to the scattering cross section. It is therefore a product of three quantities: the average intensity of the neutron beam at the sample, of the average efficiency of the neutron detector at these scattering angles, and of the solid angle comprising this range of scattering angles. We determined this distribution by treating the H_2O scattering as a secondary calibration standard.

The reasonable assumption that the Paalman–Pings attenuation coefficients at low Q, are constant with scattering angle enabled us to calculate the attenuation corrections from measurements of the transmitted intensity. For example, in the case of the measurement of $I_{SC}(Q, t)$, the overall attenuation of the sample single-scattering, $A_{S,SC}$, and container single-scattering, $A_{C,SC}$, are identical and equal to the fraction of neutrons transmitted by the sample and container.

Similarly, by reference to transmission measurements, the scattered intensity from the water calibration sample was corrected for the contribution of the silica container. The resulting distribution, $I_{H_2O}(Q)$ was a measure of the detector response from the uniform scattering of natural water.

4.1. Normalization

In order to obtain absolute measurements of the structure factor, $S(Q, t)$, from D_2O, the H_2O sample was treated as a secondary calibration standard to the incoherent scattering cross-section of vanadium. Energy-resolved neutron scattering measurements from an identical water sample and a vanadium slab, performed by Ghosh and Rennie [13], were employed for this purpose. With a knowledge of the energy distribution of scattered neutrons from the water sample (relative to the predominantly elastic scattering from vanadium) and of the relative energy-dependent efficiency of the D22 ^{3}He-detector, it was possible to estimate the response of the D22 detector.

The constant, C, relating the level of scattering from a 1 mm H_2O sample to an absolute scattering cross section, was obtained by interpolating results from inelastic scattering measurements at the incident wavelengths $\lambda = 5$ Å and $\lambda = 8$ Å, and at constant scattering angle $\theta = 4^\circ$. This permitted us to define the calibration function, $\Phi(Q)$, as follows:

$$\Phi(Q) = (CN_{H_2O})^{-1} I_{H_2O}(Q)$$

where $C = 8.01$ barn sr^{-1} ($\pm 10\%$) and N_{H_2O} is the total number of water molecules in the beam.

4.2. Instrumental resolution

The RMS width of the instrument resolution function, $\Delta Q(Q)$, is assumed to contain a Q-independent contribution from the geometry of the instrument layout and a Q-dependent contribution from the acceptance of the wavelength selector. We measured the first contribution from the profile of the attenuated transmitted beam at the detector, with a full-width-half-maximum value:

$$\Delta Q_0 = 4.7 \times 10^{-3} \text{ Å}^{-1}(\text{FWHM}).$$

The incident wavelength distribution is obtained from the D22 instrument specifications [14], derived originally from time-of-flight measurements, $\Delta\lambda/\lambda = 0.1$ (FWHM). From these values we obtain the resulting expression for the width of the resolution function:

$$(8 \ln 2)\Delta Q^2(Q) = (\Delta Q_0)^2 + (Q\Delta\lambda/\lambda)^2.$$

We use the following expression, given in Pedersen *et al* [15], for a Gaussian-profile resolution function at a flat-plate detector, in radially regrouped data sets:

$$R(Q', Q) = \frac{Q'}{\Delta Q^2(Q)} \exp\left(-\frac{Q'^2 + Q^2}{\Delta Q^2(Q)}\right) I_0\left(\frac{Q'Q}{\Delta Q^2(Q)}\right)$$

where $I_0(x)$ is the modified Bessel function of first kind and zero order.

This gives the following expression for the Ornstein–Zernike equation convoluted with the instrument resolution function:

$$S(Q,t) = \int_0^{Q_{\max}} R(Q', Q) \frac{S(0,t)}{1 + \xi(t)^2 Q'^2} \, \mathrm{d}Q' \tag{6}$$

which must be integrated numerically.

4.3. Curve-fitting procedure

The experimental scattering data $I_{SC}(Q,t)$ at each state point, t, was modelled with equation (5) and equation (6). Least-squares curve fitting procedures were performed with $\xi(t)$, $S(0,t)$ and M_{SC} as the free parameters. An iterative and self-consistent process was employed to restrict the range of momentum transfer treated by the fitting procedure to $0 < Q < x/\xi(t)$, where x was chosen to be 4. We also verified that other values of x in the range $1 < x < 8$ did not alter significantly the results obtained, except that reducing the number of data points increased noise in the values of the fitted parameters.

5. Results and discussion

Examples of the experimental structure factor, $S(Q;t)$, with correct background subtraction, are shown in figure 2. It is clear that for these results the Ornstein–Zernike equation provides a good description of the scattered intensity.

The temperature dependences of the parameters in equation (1) are shown in figures 3 and 4. The reduced temperature, t, was calculated from an assumed critical temperature, comprising the systematic errors mentioned above, that produced the closest fit to simple power-law behaviour in the variable $\xi(t)$. However, it was found that a range of assumed critical temperatures (approximately 0.1 K) could be chosen to give an acceptable fit; each giving a corresponding range of critical exponents and amplitudes. This enabled us to estimate additional experimental errors due to our inability to determine the exact value of the critical point that corresponds to the disappearance of the meniscus on phase coexistence. It was also noted that the critical temperature obtained by the criterion of obtaining the best fit to a power law in $\xi(t)$ does not appear to coincide with the temperature at which the maxima in $\xi(t)$ and $S(0,t)$ were observed. As can be seen from figures 3 and 4, both parameters appear to have maxima at $t = 0.0003$ rather than $t = 0$. Consequently, only at values of $t > 0.0008$ do power-law equations appear to provide a good description of the behaviour of $\xi(t)$ and $S(0;t)$. This discrepancy may be an artefact caused by limitations due to temperature gradients in the container with the result that we are unable to resolve state points with values $t < 0.0008$.

From the representation of the temperature dependence of the correlation length and long wavelength limit of the structure factor in equation (3) and equation (4) we obtain values for the critical amplitudes as follows: $\xi_0 = 1.30 \pm 0.23$ Å, $k_B T_c n_c p_c^{-1} \Gamma = 1.20 \pm 0.32$; and for the critical exponents as: $\nu = 0.62 \pm 0.03$, $\gamma = 1.14 \pm 0.05$. This may be compared with the values $\nu = 0.630$, $\gamma = 1.242$, from theory; $k_B T_c n_c p_c^{-1} \Gamma = 0.802$ from the Ising-like scaled equation of state due to Kamgar-Parsi *et al* [7]; and $\xi_0 = 1.28$ Å from the hypothesis of two-scale factor universality [11] and the scaled equation of state. Clearly, the parameters we obtained for the power-law description of $\xi(t)$ are in excellent agreement with the theoretical predictions based on the scaled equation of state. We have therefore shown that the predictions of the hypothesis of two-scale factor universality [11] are valid on the critical isochore. On the other hand, the parameters obtained for the power-law behaviour of $S(0,t)$ on the critical isochore are not in such good agreement. This is due to errors, which could be as large as

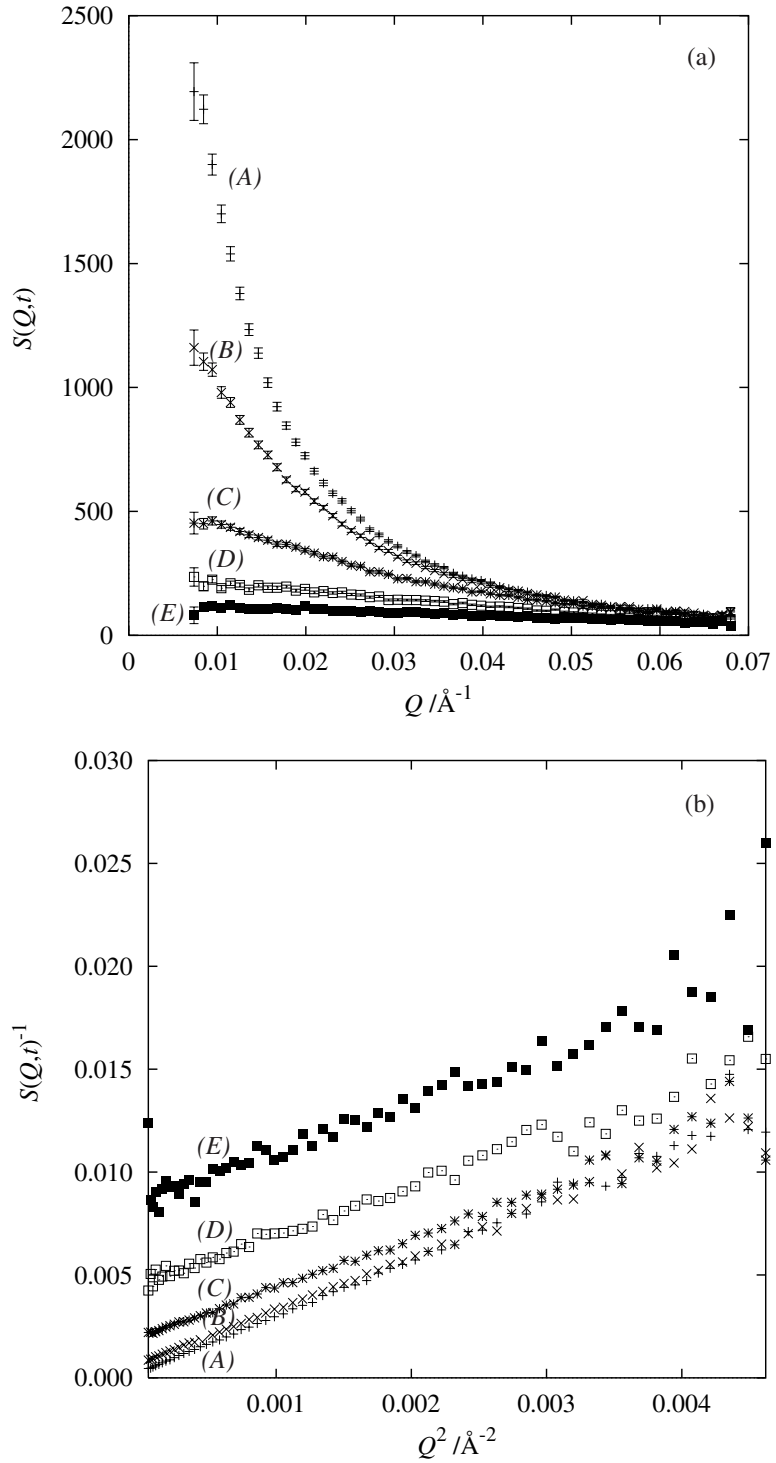

Figure 2. (a) Structure factors $S(Q, t)$ along the critical isochore at five state points: (A) $t = 0.001\,01$, (B) $t = 0.002\,14$, (C) $t = 0.005\,12$, (D) $t = 0.010\,97$, (E) $t = 0.018\,97$. (b) The corresponding Ornstein–Zernike plots of data in figure 2(a).

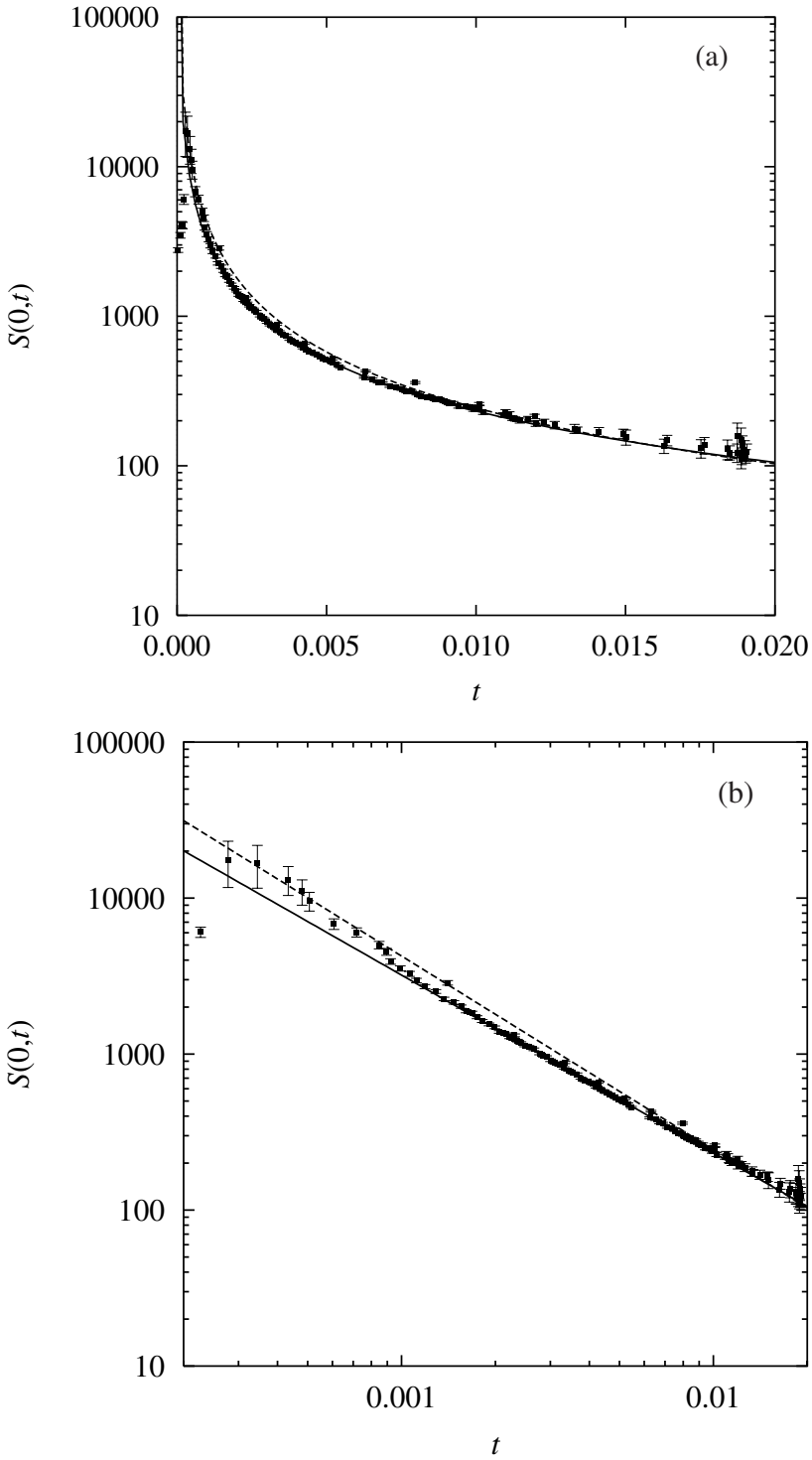

Figure 3. Temperature dependence of $S(0, t)$ with curves of power-law behaviour obtained from this experiment (solid line) and from a 3D-Ising-like scaled equation of state [7] (dashed line). (a) Linear axis in t. (b) Logarithmic axis in t.

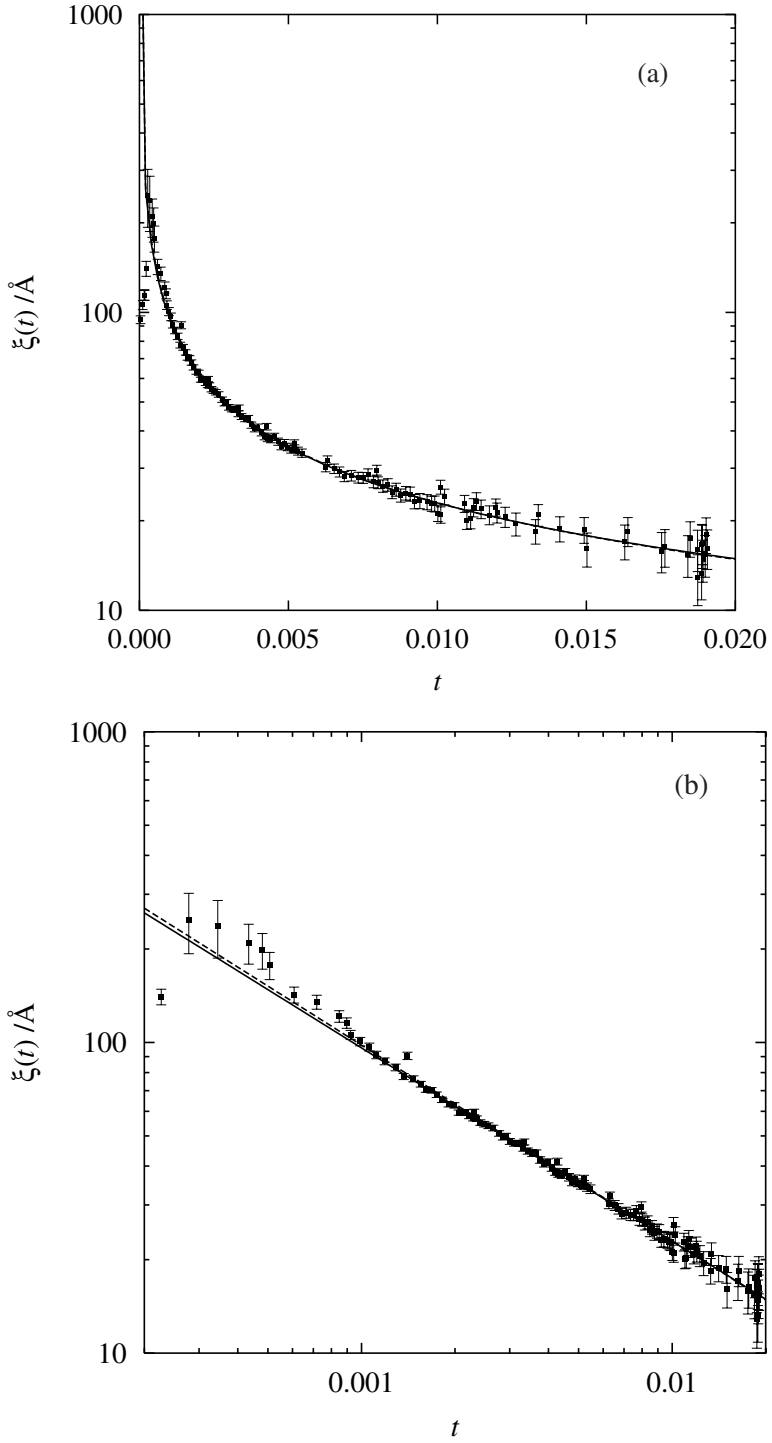

Figure 4. Temperature dependence of $\xi(t)$ with curves of power-law behaviour obtained from this experiment (solid line) and from a 3D-Ising-like scaled equation of state [7] according to the hypothesis of two-scale factor universality (dashed line). (a) Linear axis in t. (b) Logarithmic axis in t.

30%, introduced in extrapolating the scattering data to $Q = 0$, inaccuracy in the normalization process and inconsistency between the integrated flux on the sample and calibration standard.

Finally, at this level of accuracy, we observed no significant deviation from the Ornstein–Zernike equation. This is unsurprising since such deviations are characterized by the exponent $\eta = \gamma/\nu - 2$, which is expected to be small and of the order of 0.02 in the 3D-Ising universality class. Experiments to determine such a value would require experimental data closer to T_c and over a range in Q that would enable one to determine deviations in the results from a purely Lorentzian form. Damay and co-workers [16] have shown that such experiments are at the limit of what is possible by SANS methods.

6. Conclusions

We have demonstrated the use of SANS as a sensitive probe of critical fluctuations in D_2O. The results show agreement in the scaling behaviour with that observed in thermodynamic measurements and as is expected from the theory of critical phenomena [1]. In particular they show that D_2O and therefore by extension H_2O belong to the three-dimensional Ising universality class of materials.

The SANS measurement described here of critical scattering in D_2O can readily be extended to aqueous electrolyte solutions, where one might anticipate some intriguing behaviour, such as has recently been observed in ionic fluids [6]. We have demonstrated that measurements of the critical exponents can be obtained without initial assumptions about the universality class. The experimental methods presented here could therefore provide relevant information about critical scaling behaviour in other aqueous solutions.

Acknowledgments

The authors are grateful to Mr B R Stockford and Mr M Deacon for their technical expertise in the construction of the equipment used in the measurements, Drs R H Tromp and P de Jong, who developed much of the early methodology of the experiments, and Dr R E Ghosh for his advice on the data analysis especially concerning data corrections for multiple scattering and instrumental resolution. They also thank EPSRC for financial assistance and ILL for the award of a studentship to DS to pursue studies towards a PhD.

Addendum

While this paper was in the review stage prior to publication, a SANS study of D_2O near its critical point was published by the Saclay Group [17]. The data collected by this group are in the Q-range $0.07 \leqslant Q(\text{Å}^{-1}) \leqslant 0.36$, and are complementary to those in the paper above. Being at larger Q, the authors used a parametric fitting procedure based on the Fisher Langer expansion to determine suitable values for ξ_0, assuming Ising-like behaviour. Overall there is excellent agreement between the two sets of information.

References

[1] Sengers J V and Levelt Sengers J M H 1978 *Progress in Liquid Physics* ed C A Croxton (New York: Wiley) p 103
[2] Wilson K G 1983 *Rev. Mod. Phys.* **55** 583
[3] See e.g. Clifford T and Bartle K 1993 *Chemistry in Britain* (London: R. Soc. Chem) p 499 and references therein
[4] See e.g. Lunacek J H and Cannell D S 1971 *Phys. Rev. Lett.* **27** 841

[5] Levelt Sengers J M H, Kamgar-Parsi B, Balfour F W and Sengers J V 1983 *J. Phys. Chem. Ref. Data* **12** 1
[6] Narayanan T and Pitzer K S 1995 *J. Chem. Phys.* **102** 8118
[7] Kamgar-Parsi B, Sengers J V and Levelt Sengers J M H 1983 *J. Phys. Chem. Ref. Data* **12** 513
[8] Egelstaff P A 1967 *An Introduction to the Liquid State* (New York: Academic)
[9] Fisher M E 1983 *Critical Phenomena (Springer Lecture Notes in Physics 186)* ed F J W Hahne (Berlin: Springer) p 1
[10] Damay P, Leclercq F and Chieux P 1989 *Phys. Rev.* B **40** 4696
[11] Privman V, Hohenberg P C and Aharony A 1991 *Phase Transitions and Critical Phenomena* vol 14 ed C Domb and J L Lebowitz (London: Academic) p 79
[12] Paalman H H and Pings C J 1962 *J. Appl. Phys.* **33** 2635
[13] Ghosh R E and Rennie A R 1999 *J. Appl. Crystallogr.* **32** 1157–63
[14] 1997 *The Yellow Book, Guide to Neutron Research Facilities at the ILL* Institut Laue-Langevin, 6 rue J Horowitz, Grenoble, France
[15] Pedersen J S, Posselt D and Mortensen K 1990 *J. Appl. Crystallogr.* **23** 321
[16] Damay P, Leclerq F, Magli R, Formisano F and Lindner P 1998 *Phys. Rev.* B **58** 12 038
[17] Bonetti M, Romet-Lemonne G, Calmettes P and Bellissent-Funel M C 2000 *J. Chem. Phys.* **112** 268